

This is a repository copy of *Using meteorological normalisation to detect interventions in air quality time series*.

White Rose Research Online URL for this paper:
<http://eprints.whiterose.ac.uk/138077/>

Version: Accepted Version

Article:

Grange, Stuart K. orcid.org/0000-0003-4093-3596 and Carslaw, David C. orcid.org/0000-0003-0991-950X (2018) Using meteorological normalisation to detect interventions in air quality time series. *Science of The Total Environment*, 653. pp. 578-588.

Reuse

This article is distributed under the terms of the Creative Commons Attribution (CC BY) licence. This licence allows you to distribute, remix, tweak, and build upon the work, even commercially, as long as you credit the authors for the original work. More information and the full terms of the licence here:
<https://creativecommons.org/licenses/>

Takedown

If you consider content in White Rose Research Online to be in breach of UK law, please notify us by emailing eprints@whiterose.ac.uk including the URL of the record and the reason for the withdrawal request.

Using meteorological normalisation to detect interventions in air quality time series

Stuart K. Grange^{a,*}, David C. Carslaw^{a,b}

^a*Wolfson Atmospheric Chemistry Laboratories, University of York, York, YO10 5DD, United Kingdom*

^b*Ricardo Energy & Environment, Harwell, Oxfordshire, OX11 0QR, United Kingdom*

Abstract

1 Interventions used to improve air quality are often difficult to detect in air quality
2 time series due to the complex nature of the atmosphere. Meteorological normalisation
3 is a technique which controls for meteorology/weather over time in an air quality time
4 series so intervention exploration (and trend analysis) can be assessed in a robust way.
5 A meteorological normalisation technique, based on the random forest machine learning
6 algorithm was applied to routinely collected observations from two locations where known
7 interventions were imposed on transportation activities which were expected to change
8 ambient pollutant concentrations. The application of progressively stringent limits on the
9 content of sulfur in marine fuels was very clearly represented in ambient sulfur dioxide (SO₂)
10 monitoring data in Dover, a port city in the South East of England. When the technique was
11 applied to the oxides of nitrogen (NO_x and NO₂) time series at London Marylebone Road (a
12 Central London monitoring site located in a complex urban environment), the normalised
13 time series highlighted clear changes in NO₂ and NO_x which were linked to changes in primary
14 (directly emitted) NO₂ emissions at the location. The clear features in the time series were
15 illuminated by the meteorological normalisation procedure and were not observable in the
16 raw concentration data alone. The lack of a need for specialised inputs, and the efficient
17 handling of collinearity and interaction effects makes the technique flexible and suitable for a
18 range of potential applications for air quality intervention exploration.

Keywords:

Air pollution, Data analysis, Management, Machine learning, Random forest

19 **1. Introduction**

20 Across all spatial and temporal scales, weather influences concentrations of atmospheric
21 pollutants and in turn ambient air quality (Stull, 1988; Monks et al., 2009). The effects
22 of weather (or meteorology) on air quality are often much greater than intervention or
23 management efforts to control air pollution and therefore intervention events can be very
24 difficult to detect and quantify within an observational record (Anh et al., 1997). Similarly,
25 when considering trends in ambient air pollution, it can be difficult to know whether a
26 change in concentration is due to meteorology or a change in emission source strength.
27 Meteorological variation can therefore frustrate the analysis of trends in different pollutant
28 species. If meteorology is not controlled or accounted for, the changes in pollutant concentra-
29 tions observed may be contaminated with meteorological variation rather than emission or
30 chemically induced perturbations which can lead to erroneous conclusions concerning the
31 efficacy of air quality management strategies (Libiseller et al., 2005; Wise and Comrie, 2005).
32 This issue is often acknowledged, but infrequently addressed.

33 Meteorological normalisation is one technique which can be used to control for meteorology
34 over time in air quality time series. The central philosophy of meteorological normalisation
35 is to reduce variability in an air quality time series with statistical modelling. The reduction
36 of variability is achieved by training a model which can explain some of the variation of
37 pollutant concentrations through a number of independent variables. The independent
38 variables used are typically surface-based meteorological observations and time variables
39 which act as proxies for regular emission patterns such as hour of day and season (Derwent
40 et al., 1995). However, in practice, any independent variable which could explain variations
41 in pollutant concentrations could be used. Once the model has been trained and it is found
42 that it can explain an adequate amount of the dependent variable's variation, the model can
43 be used to remove the influence the independent variables have on the dependent variable
44 by sampling and predicting. The time series which results can then be exposed to further
45 exploratory data analysis (EDA) techniques such as formal trend analysis and/or intervention

*Corresponding author

Email address: `stuart.grange@york.ac.uk` (Stuart K. Grange)

46 exploration ([Grange et al., 2018](#)). The normalised time series is in the pollutant’s original
47 units and can be thought of as concentrations in “average” or invariant weather conditions.

48 There has been some air quality research conducted which uses the idea of change-point
49 analysis to investigate changes in atmospheric pollutant concentrations (for example [Carslaw
50 et al., 2006](#); [Carslaw and Carslaw, 2007](#)). Methods such as these rely on regime changes
51 where a time series abruptly shifts from one regime to another ([Lyubchich et al., 2013](#)).
52 In the air quality domain, this rarely happens, since changes are usually nuanced and
53 occur progressively with much variability which makes the generality of this approach for
54 investigating intervention efforts poor. Meteorological normalisation is potentially a more
55 general approach which enables its use in a greater range of applications.

56 Atmospheric processes are complex, non-linear, and observations commonly record
57 collinearity with other observations. These attributes make the process of statistical mod-
58 elling very challenging, especially so with parametric methods ([Barnpadimos et al., 2011](#)).
59 With the rise of machine learning algorithms, these attributes can be much more easily
60 accommodated due to the non-parametric and robust nature of these techniques ([Friedman
61 et al., 2001](#)). The meteorological normalisation technique used here uses random forest, an
62 ensemble decision tree machine learning method as the modelling algorithm.

63 Random forest has been described very well and in depth elsewhere (see [Breiman, 2001](#);
64 [Friedman et al., 2001](#); [Tong et al., 2003](#); [Ziegler and König, 2013](#); [Jones and Linder, 2015](#);
65 [Grange et al., 2018](#)). However in brief, a single decision tree is formed from a series of
66 binary splits which results in homologous or “pure” groups. The splitting process is recursive
67 which means splitting occurs until purity is achieved if the tree is allowed to grow to its
68 maximum depth. Decision trees make no assumptions on the input data structure (they
69 are non-parametric), allow for interaction and collinearity among variables, and will ignore
70 variables which are irrelevant to the dependant variable ([Ziegler and König, 2013](#)). Decision
71 trees are fast to train, fast to make predictions, and are conceptually simple to understand.
72 However, they suffer heavily from overfitting, an issue where the model represents the training
73 set well, but does not generalise to sets which were not used for training ([Jones and Linder,
74 2015](#)). Using a model which predicts pollutant concentrations and suffers from overfitting

75 would result in the model being contaminated with noise from the training set and unreliable
76 predictions would impede analyses.

77 Random forest is an algorithm which controls for the tendency of decision trees to overfit.
78 The algorithm achieves this by sampling (with replacement) the training set with a process
79 called bagging (bootstrap aggregation) ([Breiman, 1996](#)). In modern usage, sampling of the
80 independent variables is usually done during bagging too. Bagging results in a new, sampled
81 set called out-of-bag (OOB) data. A decision tree is then grown on the OOB data. The
82 bagging-then-tree growth is repeated, generally a few hundred times. Because OOB data is
83 sampled, all the decision trees are grown on differing observations and independent variables
84 which leads to a “forest” of decorrelated trees. After training, all the individual trees within
85 the forest are used to predict, but their predictions are aggregated as a mean (or the mode
86 for categorical dependent variables) and that forms the single ensemble prediction for the
87 model.

88 The meteorological normalisation technique is pragmatic in respect to the input variables
89 required for many common applications. Generally, routinely accessible surface meteorological
90 variables are very effective for the process and specialised or obscure variables are generally
91 not necessary for the technique to be applied. Although traffic counts, upper air data,
92 and outputs from weather models will usually strengthen a model’s explanatory power, the
93 existence or access to such variables is not a prerequisite, an attribute which is very useful
94 for most situations where such inputs are not available. For pollutants which are primarily
95 controlled by regional scale processes, most notably particulate matter (PM) and ozone
96 (O_3), additional variables such as boundary layer height, air mass cluster, or back trajectory
97 information would however be beneficial to include if possible and examples can be found
98 elsewhere, for example [Grange et al. \(2018\)](#).

99 The temporal variables used as independent variables in the meteorological normalisation
100 models: Julian day, weekday, and hour of year are included not for their direct influence on
101 atmospheric concentrations, but because they act as proxies for cyclical emission patterns.
102 Hour of day for example offers a term to explain emissions with a diurnal cycle such as
103 traffic-related rush hour emissions or domestic heating phases, while Julian day is a seasonal

104 term which represents emissions or atmospheric chemistry which varies seasonally. These
105 processes are generally strong drivers of concentrations of most atmospheric pollutants
106 (Henneman et al., 2015). Random forest’s ability to handle collinearity and interaction
107 between these and the other independent variables used and the lack of need of specialised
108 or exotic inputs results in a flexible tool kit for probing the influences of interventions on air
109 quality time series.

110 *1.1. Objectives*

111 The primary objective of this paper is to apply a meteorological normalisation technique
112 based on random forest, a machine learning algorithm to detect interventions in air quality
113 monitoring data. This is done to gain understanding of what physical and chemical processes
114 are driving ambient pollutant concentrations and highlight the suitability and potential of
115 the technique to other applications.

116 Two case studies are presented using routine data sets in Dover, South East England
117 where sulfur fuel limits of ships were imposed and changes in ambient sulfur dioxide (SO₂)
118 concentrations are expected and in Central London where congestion charging and local bus
119 fleet management has perturbed oxides of nitrogen (NO_x) emission sources. The changes in
120 concentrations and emissions are then explained in respect to implementation of policy which
121 would be difficult to detect with other EDA techniques where no meteorological normalisation
122 is performed.

123 **2. Methods**

124 *2.1. Data*

125 *2.1.1. Port of Dover SO₂*

126 Hourly SO₂ concentrations were analysed from the Port of Dover, a major port located in
127 Kent in the South East of England. Two air quality monitoring sites, Dover Docks and Dover
128 Langdon Cliff’s SO₂ data were queried from the Kent Air Quality database (Ricardo Energy
129 & Environment, 2018). A nearby meteorological site, Langdon Bay located to the west of
130 the port was used to provide surface meteorological observations and were accessed from

131 NOAA’s Integrated Surface Database (ISD) (NOAA, 2016) (Figure 1(a)). The monitoring
 132 sites had different commissioning and decommissioning dates and neither site is still operating
 133 (Table 1). SO₂ observations are available between March 2001 and December 2012. The
 134 data capture rates for SO₂ at Dover Langdon Cliff and Dover Docks for their online period
 135 were 92 and 82 % respectively. These monitoring sites are of interest because marine fuels
 136 in British and European waters have been subject to a series of sulfur content fuel limits.
 137 The introduction and continued enforcement of these sulfur fuel limits were expected to
 138 influence ambient SO₂ concentrations. The details of these interventions are discussed further
 139 in Section 3.1.2.

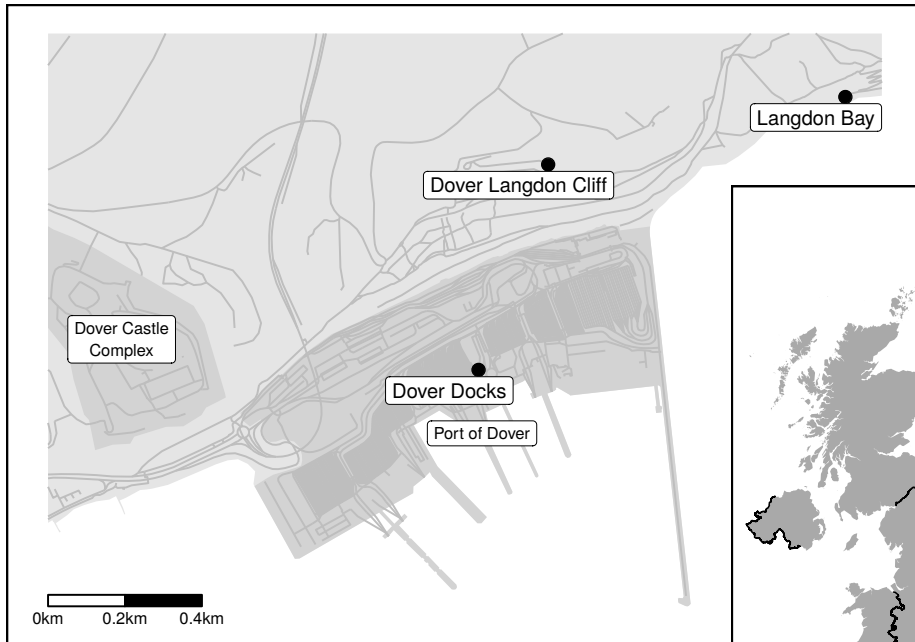
Table 1: Details of the air quality monitoring sites in Dover and London used in this analysis. Sites without end dates are still operational.

Location	Site name	Site type	Latitude	Longitude	Elevation	Date start	Date end
Dover	Langdon Bay	Meteorological	51.133	1.350	117	1973-03-08	
Dover	Dover Langdon Cliff	Urban background	51.132	1.339	98	2001-03-17	2010-03-05
Dover	Dover Docks	Urban industrial	51.127	1.336	6	2006-11-17	2013-01-03
London	London Heathrow	Meteorological	51.478	-0.461	25	1948-12-01	
London	London Marylebone Road	Traffic	51.523	-0.155	35	1997-01-01	

140 2.1.2. London Marylebone Road NO₂ and NO_x

141 Hourly NO₂ and NO_x data from London’s Marylebone Road air quality monitoring site
 142 were accessed from **smonitor** Europe, a European database containing the observations
 143 and metadata from the AirBase and Air Quality e-Reporting (AQER) repositories (Grange,
 144 2016, 2017). NO_x concentrations have been monitored since July 1997 and the final year of
 145 reporting sourced from the European data repositories used was 2016. Data capture rates for
 146 NO_x and NO₂ for the analysis period were 97 %. London Heathrow, a large airport located
 147 at the far west of Greater London was used for surface meteorological observations sourced
 148 from NOAA’s ISD (Figure 1(b)). London Marylebone Road is situated in a complicated
 149 central urban environment. The site is located one metre south of the kerb on the A501
 150 trunk road and sits within an irregularly shaped street canyon. London Marylebone Road is
 151 a prominent and often analysed site due to its long observational record and diverse suite of

(a) Dover



(b) Greater London

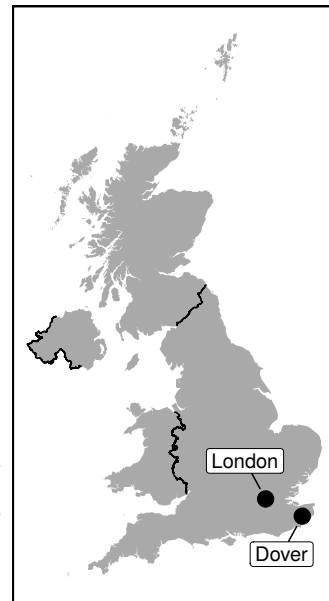
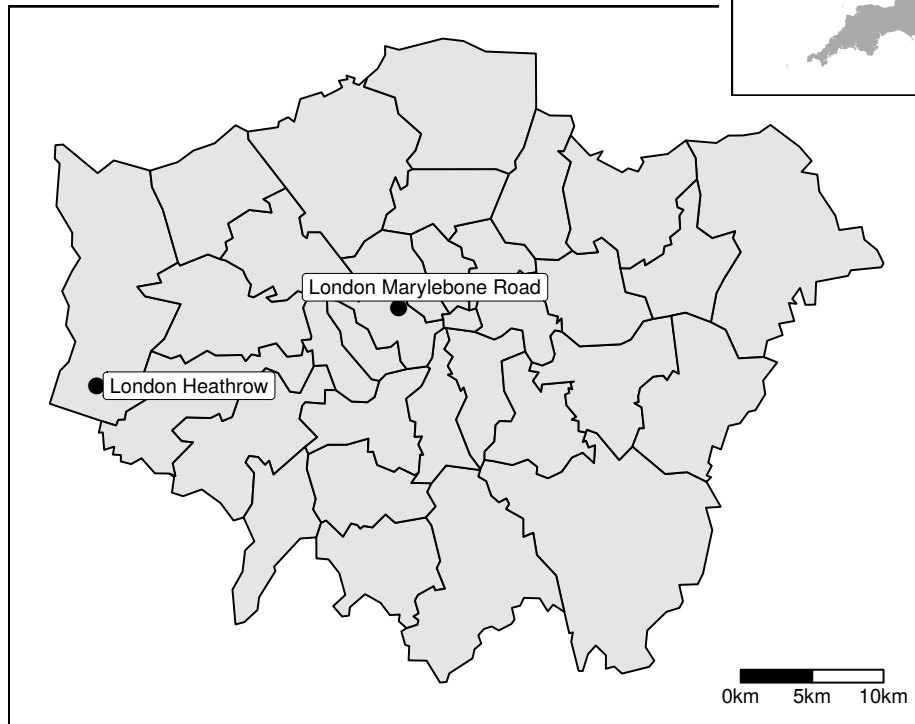


Figure 1: Maps of the study sites with a United Kingdom insert for country-scale context. The Port of Dover complex is displayed in (a) and the internal lines indicate roads and Greater London is shown in (b), with the London Boroughs and City of London indicated with internal polygons.

152 pollutants which are monitored at the site (Jeanjean et al., 2017).

153 NO_x and NO₂ concentrations across European cities are a significant issue and many
154 member states are non-compliant to the legal European ambient air quality limits (Weiss
155 et al., 2012; Grange et al., 2017). Almost all locations which are non-compliant are classified
156 as roadside (or ‘traffic-influenced’) (European Environment Agency, 2016). London has some
157 of the highest roadside concentrations of NO_x and NO₂ in Europe and London Marylebone
158 Road (Figure 1(b)) is an often referenced monitoring site for its high concentrations.

159 To combat the issue of traffic congestion, Greater London authorities imposed the
160 Congestion Charge Zone (CCZ), which was first enforced in February 2003 (Atkinson
161 et al., 2009). Since that time, the London Low Emission Zone (LEZ), and the Emissions
162 Surcharge (better known as the T-Charge) have also been implemented to combat air pollution
163 (Transport for London, 2018). The details and start dates of these various measures are
164 displayed in Table 2. All these interventions are significant investments with large amounts
165 of planning and resources to execute and maintain.

Table 2: Details of interventions within Greater London to counter traffic congestion.

Name	Abbreviation	Start date	Area covered	Operation
Congestion Charge Zone	CCZ	2003-02-17	Central London	07:00–18:00 Mo-Fr
London Low Emission Zone (first phase)	LEZ	2008-02-04	Greater London	24/7
London Low Emission Zone (second phase)	LEZ	2012-01-03	Greater London	24/7
Emissions Surcharge	T-Charge	2017-10-23	Central London	07:00–18:00 Mo-Fr
Ultra Low Emission Zone (planned)	ULEZ	2019-04-08	Central London	24/7

166 2.2. Modelling and the hyperparameters

167 For both examples, the meteorological normalisation procedure was conducted in the
168 same way and the **rmweather** R package (version 0.1.2) was used for this process (R Core
169 Team, 2018; Grange, 2018). The number of trees for the random forest models was fixed at
170 300, the minimal node size was five, and the number of variables split at each node was the
171 default for regression mode: the rounded down square root of the number of independent
172 variables which in these examples was three (**rmweather**’s function arguments `n_trees`,

173 `min_node_size`, and `mtry` respectively). The independent variables used were: Unix date
174 (number of seconds since 1970-01-01) as the trend term, Julian day as the seasonal term,
175 weekday, hour of day, air temperature, relative humidity, wind direction, wind speed, and
176 atmospheric pressure. Training was only conducted on observations which had non-missing
177 wind speed and the pollutant being modelled. Three hundred predictions were used to
178 calculate the meteorologically normalised trend. The normalised trends were aggregated
179 to monthly resolution for presentation in Section 3. A conceptual representation of the
180 meteorological normalisation processes is displayed in Figure A1.

181 For the Dover SO₂ examples, models were calculated using the full observational set, but
182 after investigating the models (discussed in Section 3.1.1), the observations were filtered to
183 wind directions which were sourced from the port and these models are the ones which were
184 used for the time series analysis (Section 3.1.2). For observations at London Marylebone
185 Road, no filtering was undertaken. In the case of London Marylebone Road, there are a large
186 number of potential events which could influence pollutant concentrations and emissions.
187 To objectively identify events, the meteorologically normalised time series were tested for
188 breakpoints or changes in structure. The structural change algorithm is described in Zeileis
189 *et al.* (2002); Zeileis *et al.* (2003) and was implemented with the **strucchange** R package.

190 The random forest algorithm does not directly offer the ability to determine error or
191 uncertainty of estimates. However, uncertainty is important to consider in many situations.
192 To enable uncertainty to be evaluated for the case studies, 50 random forest models were
193 grown for each example with the hyperparameters described above, but with randomly
194 sampled (bootstrapped) input sets. The bootstrapping of the observational data ensured
195 the models were grown on different training sets. The importance values (a measure of the
196 variables' strength or influence on prediction), partial dependencies, and predictions for each
197 of the 50 models were then summarised. The summaries used from the "ensemble of the
198 ensembles" were the mean, and the 2.5 % and 97.5 % quantiles of the 50 estimates *i.e.* a
199 range that spans the 95 % confidence interval in the mean. The model performance statistics
200 for the four sets of models are displayed in Table 3.

Table 3: Mean random forest model performance statistics for the four sets of models grown for the analysis.

Location	Model	n	R^2
Dover	Dover Docks SO ₂	34224	0.67
Dover	Dover Langdon Cliff SO ₂	53535	0.63
London	London Marylebone Road NO ₂	131677	0.82
London	London Marylebone Road NO _x	131677	0.83

201 3. Results and discussion

202 3.1. Port of Dover SO₂

203 3.1.1. Models

204 The random forest models grown for SO₂ at the two Dover sites had R^2 values of 63 and
 205 67 % (Table 3), therefore, the models had moderate explanatory ability for Dover’s SO₂
 206 concentrations. However, it should be noted that predicting concentrations over such short
 207 time periods with intermittent source strength is challenging and data capture was less than
 208 ideal for these monitoring sites. The moderate performance can be explained by SO₂ at this
 209 location containing large amounts of variation due to ship movements and if winds were in a
 210 favourable direction to transport emissions from the port complex to the monitoring sites
 211 (southerlies). Indeed, wind direction was the most important variable for SO₂ explanation
 212 for the random forest models (Figure 2).

213 Partial dependence plots of decision tree models allow the learning process to be interpreted
 214 and a data user to examine how variables are being handled in the predictive model. Figure 3
 215 demonstrates a two-way partial dependence plot for SO₂ concentrations at Dover Landon
 216 Cliff using wind direction and date (the trend term) as the independent variables. The
 217 feature which is most clear is the band of increased SO₂ dependence between 150 and
 218 210 degrees. Outside of this band of southerly winds, there were low levels of dependence
 219 on SO₂ concentrations. The Dover Landon Cliff monitoring site was located north of the
 220 Port of Dover docks and very slightly to the east (Figure 1(a)). The partial dependence
 221 on wind direction is consistent with this location and indicates that wind direction was

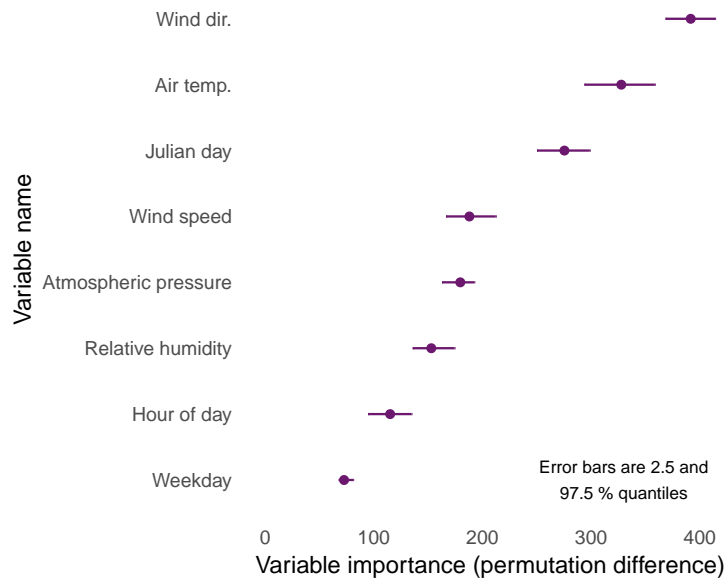


Figure 2: Variable importance plot for SO₂ at Dover Langdon Cliff between 2001 and 2010 calculated by 50 random forest models.

222 handled sensibly in the random forest model. This observation can be confirmed further
 223 with a bivariate polar plot of mean SO₂ concentrations by wind direction and speed at the
 224 monitoring site (Figure 4). The first sulfur content fuel change in mid-August 2006 can also
 225 be seen in the two-way partial dependence plot as a clear reduction in SO₂ dependence when
 226 winds were sourced from the port (the south; discussed further in Section 3.1.2; Figure 3).

227 Another clear feature isolated by the partial dependence plots was that SO₂ concentrations
 228 increased with increasing air temperature at the Dover monitoring sites (Figure 5). This
 229 relationship was an unexpected outcome because generally, pollutant concentrations are
 230 inversely related to air temperature because emissions are more efficiently diluted during
 231 warmer periods owing to increased thermal turbulence. For some sources such as heating,
 232 emissions are greater at lower temperatures, but when considering shipping emissions,
 233 this would be negligible. At Dover, the SO₂ relationship between concentrations and air
 234 temperatures was indicative of convective thermal mixing being an important physical process
 235 which resulted in SO₂ emitted by ships to be mixed towards the measurement site at the
 236 cliff top. This turbulent mixing at high temperatures resulted in high SO₂ concentrations at

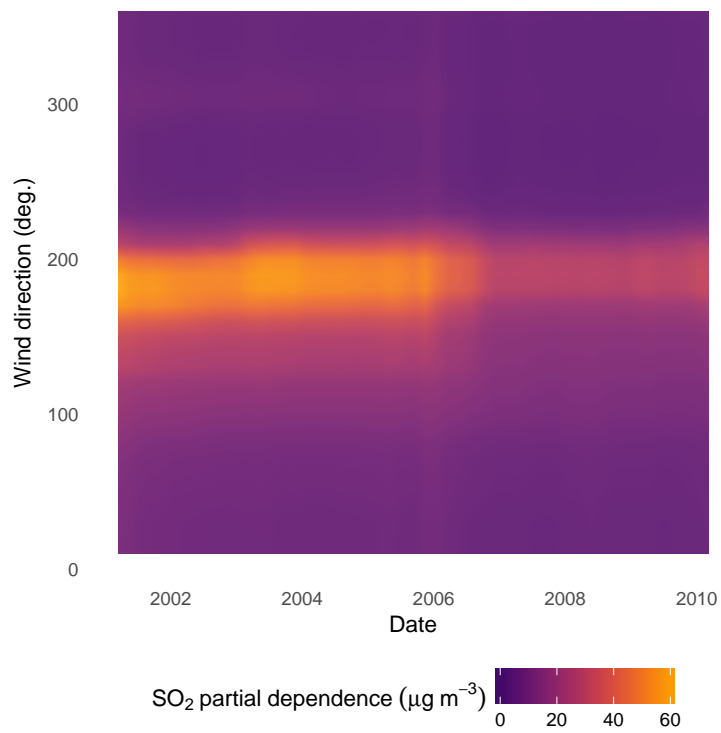


Figure 3: Partial dependence of wind direction and date on SO₂ concentrations at Dover Landon Cliff between 2001 and 2010. The Dover Landon Cliff monitoring site was located north of the Port of Dover (Figure 1(a)).

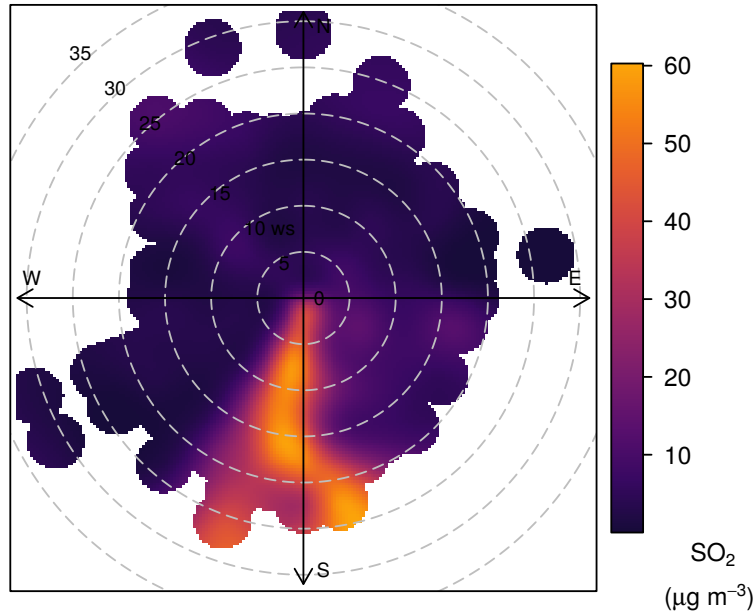


Figure 4: Bivariate polar plot of mean hourly SO_2 concentrations at Dover Landon Cliff between 2001 and 2010. The Dover Landon Cliff monitoring site was located north of the Port of Dover (for a location map, see Figure 1(a)).

237 the surface and this feature cannot be easily observed in the hourly observational data. The
 238 illumination of such physical processes is a major advantage of the random forest algorithm
 239 compared to other machine learning methods such as support vector machines (SVM) or
 240 artificial neural networks (ANNs) because they do not offer the same amount of model
 241 legibility.

242 3.1.2. Influence of sulfur fuel limits on SO_2 concentrations

243 Since the early 2000s, there has been a number of increasingly stringent sulfur based fuel
 244 limits imposed on ships operating in British and European Union (EU) waters due to their
 245 status as Sulfur Emission Control Areas (SECAs) or Emission Control Areas (ECAs). The
 246 most important events for sulfur control were implemented on August 11, 2006 and January
 247 1, 2010. In August 2006, the MARPOL Annex IV regulations were applied which introduced
 248 a 1.5 % sulfur limit on fuel oils used by vessels moving between EU ports ([International
 Maritime Organization, 2005](#)). The pre-August 2006 sulfur content for British vessels has
 249 been estimated at 2.7 % which represents a reduction in sulfur content of 44 % ([Entec, 2010](#)).
 250

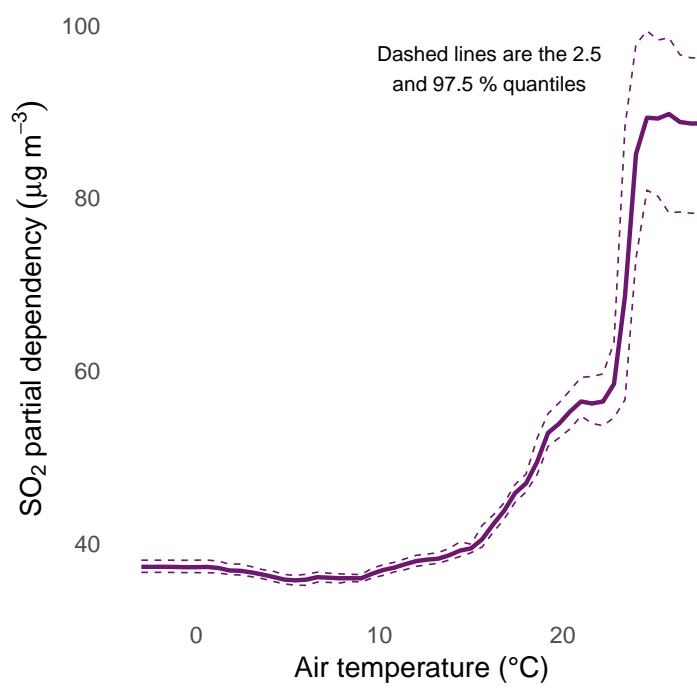


Figure 5: Partial dependence of SO₂ on air temperature at Dover Landon Cliff between 2001 and 2010 calculated by 50 random forest models.

251 At the start of 2010 an additional limit was imposed for all vessels at berth where such
252 vessels were required to be operated with maximum fuel sulfur content of 1 %. These changes
253 should be evident in the SO₂ time series of the nearby ambient monitoring sites. However, if
254 a time series is plotted, the influence of these changes are subtle and not clear due to the
255 high amounts of variation within SO₂ concentrations (Figure 6).

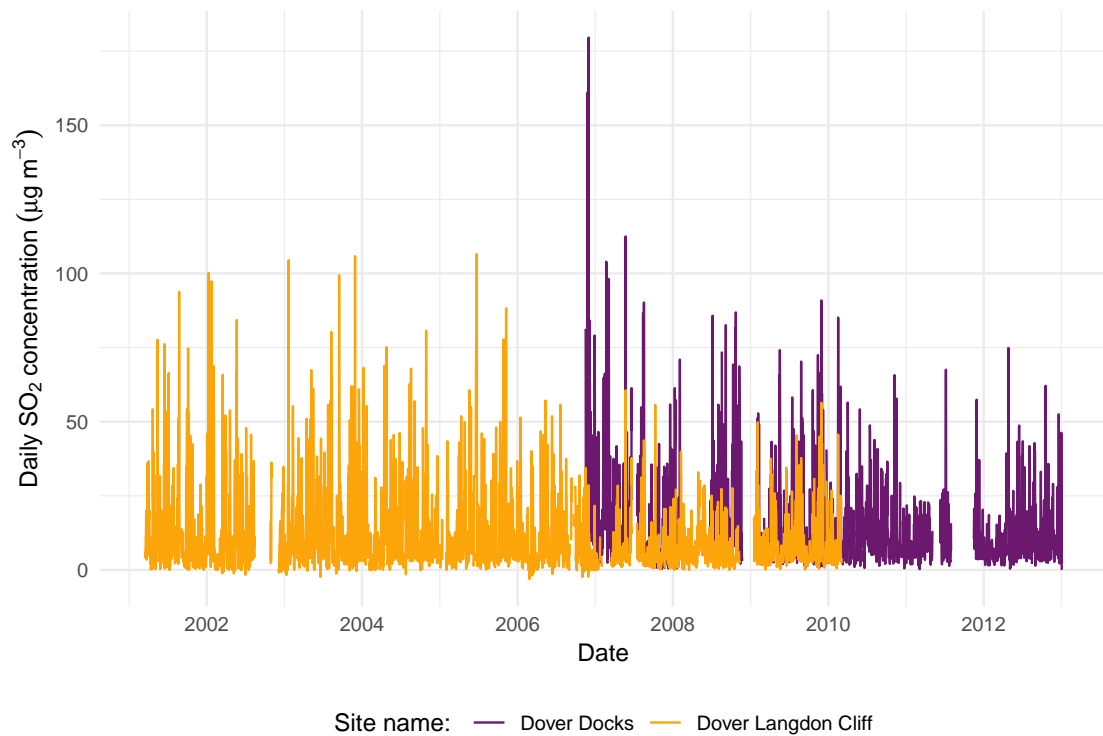


Figure 6: Daily SO₂ concentrations at two monitoring sites in Dover between 2001 and 2012.

256 The meteorologically normalised SO₂ time series for the Dover sites are displayed in
257 Figure 7, after the observations were filtered to wind directions which came for the port,
258 hence the tight 95 % confidence intervals. The dates when changes in sulfur fuel content
259 were implemented are displayed as vertical lines in Figure 7 and the influence of sulfur fuel
260 changes are clear (compared with Figure 6).

261 At Dover Langdon Cliff, the monitoring site which was online during the MARPOL
262 1.5 % fuel sulfur limit transition during August 2001 shows the shift in ambient SO₂ very
263 clearly (Figure 7). The mean meteorologically normalised SO₂ concentrations for the pre- and

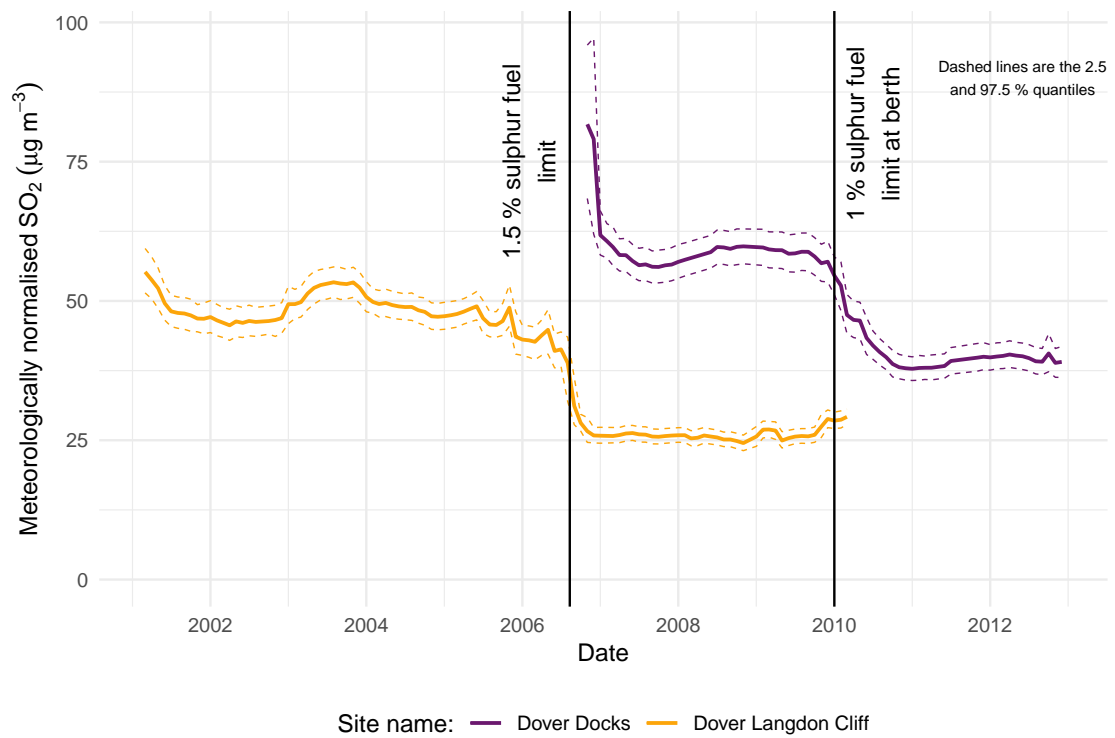


Figure 7: Meteorologically normalised SO₂ concentrations at two monitoring sites in Dover between 2001 and 2012 as calculated by 50 random forest models. The vertical lines show the start dates of when changes in marine sulfur fuel content were implemented.

264 post-fuel change periods were 48 and 26 $\mu\text{g m}^{-3}$ respectively. This difference represented in
265 percentage change is 45 % and the corresponding estimated change in sulfur fuel content was
266 44 %. This extremely good agreement between sulfur content fuel changes and normalised
267 ambient SO_2 concentrations suggests that the Port of Dover activities and ship movements
268 remained constant during the transition phase and the source of SO_2 at this location was
269 almost exclusively from the port.

270 The second sulfur fuel content change was implemented on January 1, 2010 and this
271 intervention is also clearly displayed in the meteorologically normalised SO_2 concentrations
272 of the Dover Docks monitoring site (Figure 7). The percentage change in fuel sulfur content
273 was 33 % and the percentage change in ambient SO_2 concentrations was 32 %. Like the
274 previous intervention, these two percentage changes match almost exactly, which is somewhat
275 surprising because the intervention was applied only to berthed vessels which would only
276 make up a component of the Port of Dover activities.

277 *3.2. London Marylebone Road NO_x*

278 *3.2.1. Models*

279 The random forest models of NO_x and NO_2 at London Marylebone Road performed well
280 and had R^2 values of 82 and 83 % respectively (Table 3). This good performance can be
281 explained by hour of day being a very good predictor for traffic flows and therefore emissions
282 at this location for these (mostly) traffic-sourced pollutants (Figure 8). The performance of
283 the random forest models would be rather difficult to achieve with dispersion or deterministic
284 models in such a complicated location. For example, the dispersion models evaluated in
285 [Carslaw et al. \(2013\)](#) struggled to represent the street canyon environment, even when traffic
286 information was taken into account. The importance plots for the London Marylebone Road
287 models also show that wind direction is the most important variable to predict NO_2 and
288 NO_x concentrations. London Marylebone Road is located in a street canyon and is subjected
289 to complex flows, including ventilation, vortices, and leeward accumulation of pollutants,
290 (primarily) dependent on wind direction ([Carslaw and Carslaw, 2007](#); [Catalano et al., 2016](#)).
291 This complexity is demonstrated in the importance of wind direction in explaining NO_x and

292 NO₂ concentrations (Figure 8) and this has been noted before at this location (Charron and
 293 Harrison, 2005; Westmoreland et al., 2007).

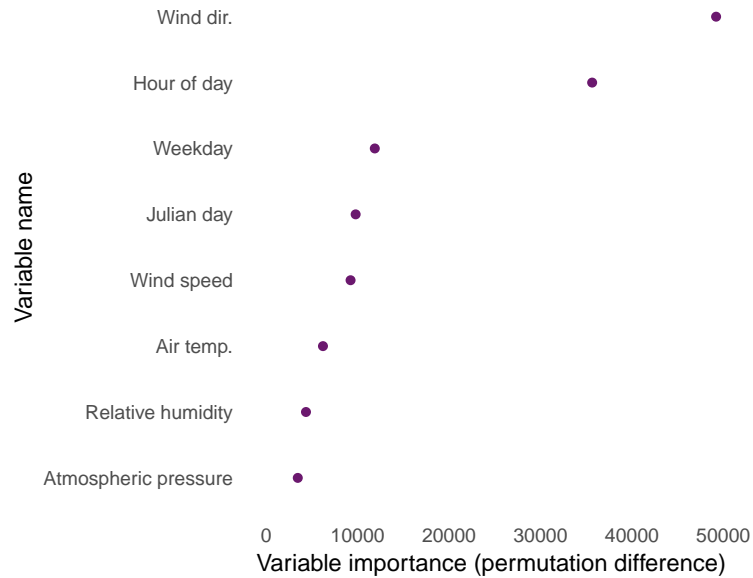


Figure 8: Variable importance plot for 50 NO₂ random forest models for London Marylebone Road. The uncertainty among the importances of the 50 models was very small and therefore the quantiles are not shown. The importances for the NO_x models were very similar.

294 3.2.2. Changes in primary NO₂

295 Using the predictive models for meteorological normalisation results in very clear and
 296 almost noiseless meteorologically normalised trends shown in Figure 9. It is immediately
 297 clear that NO_x and NO₂ are not behaving the same way at this monitoring location. This is
 298 because of changes in vehicular primary (directly emitted) NO₂ during the analysis period
 299 (1997–2016) (Carslaw, 2005; Carslaw et al., 2016; Grange et al., 2017). The vertical lines on
 300 Figure 9 show the breakpoints identified by structural change analysis after the meteorological
 301 normalisation procedure.

302 NO_x concentrations decreased after the introduction of a bus lane adjacent to the
 303 monitoring site in 2001 but have remained near constant since the introduction of the CCZ in
 304 February 2003 (Figure 9 and Table 2). Despite the progressively stringent vehicular emission

305 controls being applied across Europe between 2003 and 2016 (the last year of data in analysis),
 306 they have had little effect to NO_x at London Marylebone Road. This observation could
 307 be, at least partly, explained by the disconnect between laboratory testing and real-world
 308 emissions of NO_x which become a public issue after the diesel emission scandal in September
 309 2015 (Brand, 2016; Schmidt, 2016). However, heavy duty vehicles are also very important to
 310 consider alongside passenger vehicles at this Central London location (Laybourn-Langton
 311 et al., 2016; Greater London Authority, 2017).

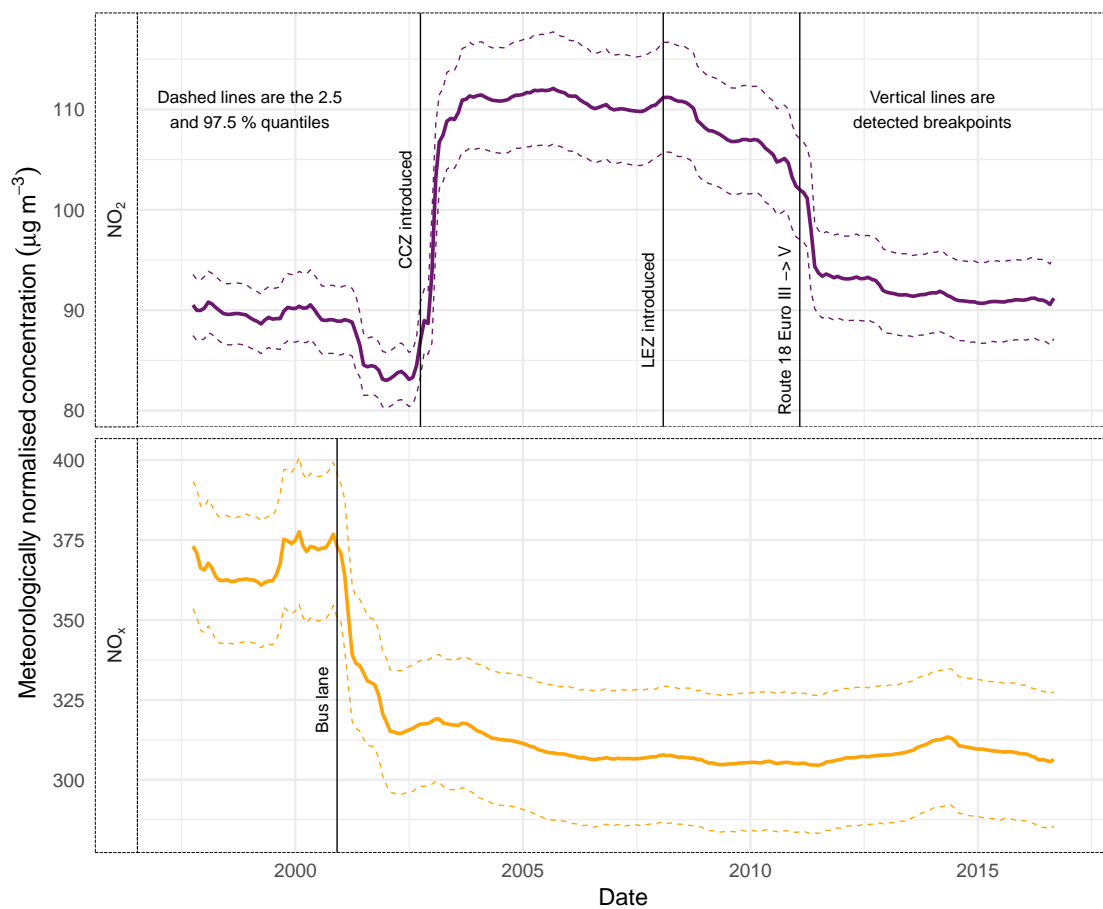


Figure 9: Meteorologically normalised NO_x and NO_2 at London Marylebone Road between 1997 and 2016 as calculated by 50 random forest models (for each pollutant). The vertical lines on show the breakpoints identified by structural change analysis.

312 NO_2 concentrations at London Marylebone Road have increased since 1997 and were at
 313 their maximum between 2002 and 2008 (Figure 9). The changes observed can be explained

314 by changes to the vehicle fleet using the adjacent A501 road resulting from the introduction
315 of congestion charging, London's Low Emission Zone, and evolution of the local bus fleet.
316 The rapid increase of NO₂ concentrations was observed in the meteorologically normalised
317 time series between July 2002 and July 2003 (Figure 9). The CCZ was introduced in mid-
318 February 2002; right in the middle of the period of increasing NO₂ and within six months
319 of the suggested breakpoint (October 2012). The increase in NO₂ concentrations was due
320 to increased primary NO₂ because no change in the meteorologically normalised NO_x was
321 observed at the same time.

322 The implementation of the CCZ was accompanied with a retrofitting programme of
323 Euro III local buses with continuously regenerating diesel particulate filters (CRDPF, also
324 known by their commercial name: CRT filters). CRDPF are passive devices and have two
325 components: an upstream oxidation catalyst and a particulate matter (PM) filter. The
326 oxidation catalyst oxidises NO within the exhaust stream to NO₂ and this NO₂ is then used
327 as a PM oxidant in the filter-proper. The observations show that these retrofitted passive
328 devices were not optimised because much of the generated NO₂ was not reduced within the
329 PM filter and was therefore emitted into the roadside atmosphere and thus significantly
330 increased ambient NO₂ concentrations (Figure 9).

331 NO₂ concentrations remained approximately stable until February 2008 when London's
332 Low Emission Zone (LEZ) was introduced and NO₂ concentrations began to decrease (Fig-
333 ure 9). The second NO₂ breakpoint was detected for February 2008 giving some evidence
334 that the LEZ reduced NO₂ concentrations at London Marylebone Road (although no corre-
335 sponding change in NO_x was observed). However, during this period the local bus fleets were
336 also being progressively replaced with newer buses compliant to the later Euro IV, V, and
337 VI heavy vehicle emission standards (Finn Coyle, Tom Cunnington, and Gabrielle Bowden
338 (Transport for London), personal communication, March 2018) as well of natural vehicle
339 turnover removing older and more polluting vehicles from the in-service fleet. The third NO₂
340 breakpoint identified coincided with route 18, the bus route with the highest peak vehicle
341 requirements (PVR), shifting from Euro III to Euro V vehicles in late 2010 (Figure 9). After
342 2011, NO₂ concentrations continued to decline with the introduction of Euro VI and hybrid

343 buses servicing the 453, 27, and 205 routes. By the end of 2016, NO₂ had declined to almost
344 pre-CCZ concentrations. The features displayed in the normalised time series were not clear
345 in the raw concentration data (displayed in Figure A2) and the breakpoints identified were
346 unable to be resolved without the meteorological normalisation technique.

347 The tandem use of the meteorological normalisation procedure and breakpoint analysis
348 is powerful and can reveal many changes, but in many cases there may not be sufficient
349 information or metadata to help explain the changes observed. In this Central London
350 example, many of the factors driving pollutant concentrations are known due to the site's
351 prominence.

352 London Marylebone Road also monitors ozone (O₃), something which is rare for roadside
353 monitoring locations in Europe. The NO₂, NO_x, and O₃ complement allows for the estimation
354 of primary NO₂ with an independent method by determining the total oxidant (OX; NO₂
355 + O₃) within NO_x (Jenkin, 2004; Carslaw and Beevers, 2005). Figure 10 shows monthly
356 estimates of the primary NO₂ fraction at London Marylebone Road with robust linear
357 regression. Figure 10 is consistent with Figure 9 with a rapid increase in primary NO₂ during
358 2002 and a reduction, but at a slower rate after 2008 thus further confirming and validating
359 that the trends observed in Figure 9 are driven by changes in primary NO₂ emissions. The
360 reason why the trend is similar in Figure 10 and Figure 9 is that at this particular site
361 increased emissions of primary NO₂ were sufficient to have a measurable effect on ambient
362 concentrations.

363 4. Conclusions

364 Controlling for changes of meteorology is an important component to consider when
365 conducting air quality data analysis over time. A meteorological normalisation technique
366 using random forest was used to investigate interventions in routine air quality monitoring
367 data from two areas. The interventions applied to marine fuel content changes were explored
368 in Dover, a port city in the South East of England and the interventions were represented in
369 the meteorologically normalised time series almost exactly. The non-black box nature of the
370 random forest models was used to investigate the dependence of pollutant concentrations

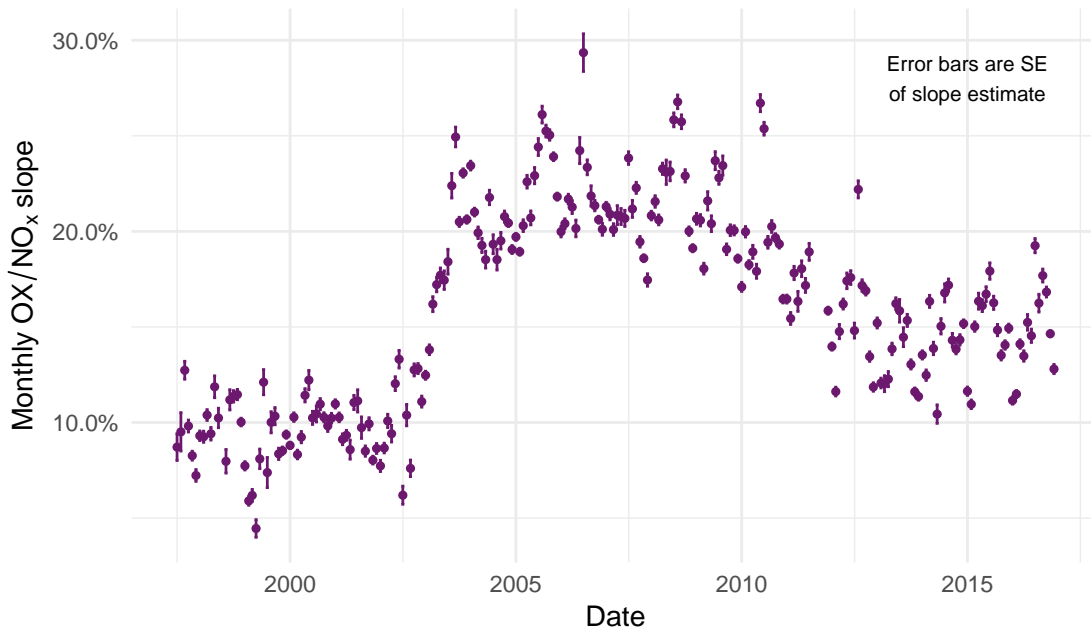


Figure 10: Monthly total oxidant (OX; $\text{NO}_2 + \text{O}_3$) at London Marylebone Road between 1997 and 2016. Slope and errors were calculated with robust linear regression.

371 on meteorological variables such as air temperature and wind direction which highlighted
 372 the benefit of the technique where physical and chemical atmospheric processes can be
 373 illuminated, understood, and explained.

374 In the example of the implementation of congestion charging in Central London, very clear
 375 changes in primary NO_2 emissions were displayed in the meteorologically normalised time
 376 series. The performance of these roadside models was high due to the models' ability to use
 377 wind direction and hour of day very effectively, something which dispersion or deterministic
 378 models struggle with when used for modelling street canyon environments. The case studies
 379 presented are both examples where there is significant ability to cross check the observed
 380 features with available information on changes in the sites' local environments to validate
 381 the outputs.

382 The meteorological normalisation technique is very relevant for exploring the influence
 383 of interventions or management activities on local air quality. The combination of a non-
 384 parametric method, the lack of need for specialised measurements, and the effective use of

385 proxy variables lends the technique to a wide range of air quality data analysis applications.

386 **Acknowledgements**

387 S.K.G. was supported by Anthony Wild with the provision of the Wild Fund Scholarship.
388 This work was also partially funded by Natural Environment Research Council (NERC)
389 [grant number: NE/N007115/1].

390 **Competing interests**

391 The authors declare no competing interest.

392 **Highlights**

- 393 • Detecting the influence of air quality interventions is important
- 394 • Changes in meteorology over time complicates air quality intervention analysis
- 395 • Meteorological normalisation was applied in two locations to explore interventions
- 396 • The changes detected in the normalised time series were associated to interventions
- 397 • The non-black-box nature of the procedure allows for interpretation of results

398 **References**

- 399 Anh, V., Duc, H., Azzi, M., 1997. Modeling anthropogenic trends in air quality data. *Journal of the Air &*
400 *Waste Management Association* 47 (1), 66–71.
401 URL <https://doi.org/10.1080/10473289.1997.10464406>
- 402 Atkinson, R., Barratt, B., Armstrong, B., Anderson, H., Beevers, S., Mudway, I., Green, D., Derwent, R.,
403 Wilkinson, P., Tonne, C., Kelly, F., Nov. 2009. The impact of the congestion charging scheme on ambient
404 air pollution concentrations in London. *Atmospheric Environment* 43 (34), 5493–5500.
405 URL <http://www.sciencedirect.com/science/article/pii/S1352231009006268>
- 406 Barmpadimos, I., Hueglin, C., Keller, J., Henne, S., Prévôt, A. S. H., Feb. 2011. Influence of meteorology on
407 PM₁₀ trends and variability in Switzerland from 1991 to 2008. *Atmospheric Chemistry and Physics* 11 (4),
408 1813–1835.
409 URL <http://www.atmos-chem-phys.net/11/1813/2011/>

410 Brand, C., 2016. Beyond ‘Dieselgate’: Implications of unaccounted and future air pollutant emissions and
411 energy use for cars in the United Kingdom. *Energy Policy* 97, 1–12.
412 URL <http://www.sciencedirect.com/science/article/pii/S030142151630341X>

413 Breiman, L., 1996. Bagging predictors. *Machine Learning* 24 (2), 123–140.
414 URL <http://dx.doi.org/10.1007/BF00058655>

415 Breiman, L., 2001. Random forests. *Machine Learning* 45 (1), 5–32.
416 URL <http://dx.doi.org/10.1023/A:1010933404324>

417 Carslaw, D., Apsimon, H., Beevers, S., Brookes, D., Carruthers, D., Cooke, S., Kitwiroon, N., Oxley, T.,
418 Stedman, J., Stocker, J., 2013. Defra Phase 2 urban model evaluation, UK AIR: Air Information Resource.
419 URL https://uk-air.defra.gov.uk/library/reports?report_id=777

420 Carslaw, D. C., Aug. 2005. Evidence of an increasing NO₂/NO_x emissions ratio from road traffic emissions.
421 *Atmospheric Environment* 39 (26), 4793–4802.
422 URL <http://www.sciencedirect.com/science/article/pii/S1352231005005443>

423 Carslaw, D. C., Beevers, S. D., Jan. 2005. Estimations of road vehicle primary NO₂ exhaust emission fractions
424 using monitoring data in London. *Atmospheric Environment* 39 (1), 167–177.
425 URL <http://www.sciencedirect.com/science/article/pii/S1352231004008775>

426 Carslaw, D. C., Carslaw, N., 2007. Detecting and characterising small changes in urban nitrogen dioxide
427 concentrations. *Atmospheric Environment* 41 (22), 4723–4733.
428 URL <http://www.sciencedirect.com/science/article/pii/S1352231007002919>

429 Carslaw, D. C., Murrells, T. P., Andersson, J., Keenan, M., 2016. Have vehicle emissions of primary NO₂
430 peaked? *Faraday Discussions* 189 (0), 439–454.
431 URL <http://dx.doi.org/10.1039/C5FD00162E>

432 Carslaw, D. C., Ropkins, K., Bell, M. C., Nov. 2006. Change-point detection of gaseous and particulate
433 traffic-related pollutants at a roadside location. *Environmental Science & Technology* 40 (22), 6912–6918.
434 URL <http://dx.doi.org/10.1021/es060543u>

435 Catalano, M., Galatioto, F., Bell, M., Namdeo, A., Bergantino, A. S., Jun. 2016. Improving the prediction of
436 air pollution peak episodes generated by urban transport networks. *Environmental Science & Policy* 60,
437 69–83.
438 URL <http://www.sciencedirect.com/science/article/pii/S1462901116300594>

439 Charron, A., Harrison, R. M., Oct. 2005. Fine (PM_{2.5}) and Coarse (PM_{2.5–10}) Particulate Matter on A
440 Heavily Trafficked London Highway: Sources and Processes. *Environmental Science & Technology* 39 (20),
441 7768–7776.
442 URL <http://dx.doi.org/10.1021/es050462i>

443 Derwent, R., Middleton, D., Field, R., Goldstone, M., Lester, J., Perry, R., 1995. Analysis and interpretation

444 of air quality data from an urban roadside location in Central London over the period from July 1991 to
445 July 1992. *Atmospheric Environment* 29 (8), 923 – 946.
446 URL <http://www.sciencedirect.com/science/article/pii/S135223109400219B>

447 Entec, 2010. Defra UK Ship Emissions Inventory—Final Report, doc Reg No. 21897-01.
448 URL [https://uk-air.defra.gov.uk/assets/documents/reports/cat15/1012131459_21897_Final_](https://uk-air.defra.gov.uk/assets/documents/reports/cat15/1012131459_21897_Final_Report_291110.pdf)
449 [Report_291110.pdf](https://uk-air.defra.gov.uk/assets/documents/reports/cat15/1012131459_21897_Final_Report_291110.pdf)

450 European Environment Agency, 2016. Air quality in Europe — 2016 report. EEA Report. No 28/2016.
451 URL <http://www.eea.europa.eu/publications/air-quality-in-europe-2016>

452 Friedman, J., Hastie, T., Tibshirani, R., 2001. *The Elements of Statistical Learning. Data Mining, Inference,*
453 *and Prediction*, 2nd Edition. Vol. 1. Springer series in statistics Springer, Berlin.

454 Grange, S. K., 2016. **smonitor**: A framework and a collection of functions to allow for maintenance of air
455 quality monitoring data.
456 URL <https://github.com/skgrange/smonitor>

457 Grange, S. K., 2017. Technical note: **smonitor** Europe. Tech. rep., Wolfson Atmospheric Chemistry
458 Laboratories, University of York.
459 URL <https://doi.org/10.13140/RG.2.2.20555.49448/1>

460 Grange, S. K., 2018. **rmweather**: Tools to Conduct Meteorological Normalisation on Air Quality Data. R
461 package version 0.1.2.
462 URL <https://CRAN.R-project.org/package=rmweather>

463 Grange, S. K., Carslaw, D. C., Lewis, A. C., Boleti, E., Hueglin, C., May 2018. Random forest meteorological
464 normalisation models for Swiss PM₁₀ trend analysis. *Atmospheric Chemistry and Physics* 18 (9), 6223–
465 6239.
466 URL <https://www.atmos-chem-phys.net/18/6223/2018/>

467 Grange, S. K., Lewis, A. C., Moller, S. J., Carslaw, D. C., Dec. 2017. Lower vehicular primary emissions of
468 NO₂ in Europe than assumed in policy projections. *Nature Geoscience* 10 (12), 914–918.
469 URL <https://doi.org/10.1038/s41561-017-0009-0>

470 Greater London Authority, 2017. London atmospheric emissions inventory (laei) 2013.
471 URL <https://data.london.gov.uk/dataset/london-atmospheric-emissions-inventory-2013>

472 Henneman, L. R., Holmes, H. A., Mulholland, J. A., Russell, A. G., Oct. 2015. Meteorological detrending
473 of primary and secondary pollutant concentrations: Method application and evaluation using long-term
474 (2000–2012) data in Atlanta. *Atmospheric Environment* 119, 201–210.
475 URL <http://www.sciencedirect.com/science/article/pii/S1352231015302521>

476 International Maritime Organization, 2005. Revised MARPOL Annex VI, annex VI of MARPOL addresses
477 air pollution from ocean-going ships.

478 URL [http://www.imo.org/en/OurWork/Environment/PollutionPrevention/AirPollution/Pages/](http://www.imo.org/en/OurWork/Environment/PollutionPrevention/AirPollution/Pages/Air-Pollution.aspx)
479 [Air-Pollution.aspx](http://www.imo.org/en/OurWork/Environment/PollutionPrevention/AirPollution/Pages/Air-Pollution.aspx)

480 Jeanjean, A. P. R., Buccolieri, R., Eddy, J., Monks, P. S., Leigh, R. J., Mar. 2017. Air quality affected by
481 trees in real street canyons: The case of Marylebone neighbourhood in central London. *Urban Forestry &*
482 *Urban Greening* 22, 41–53.

483 URL <http://www.sciencedirect.com/science/article/pii/S1618866716303740>

484 Jenkin, M. E., Sep. 2004. Analysis of sources and partitioning of oxidant in the UK—Part 2: contributions
485 of nitrogen dioxide emissions and background ozone at a kerbside location in London. *Atmospheric*
486 *Environment* 38 (30), 5131–5138.

487 URL <http://www.sciencedirect.com/science/article/pii/S1352231004006193>

488 Jones, Z., Linder, F., 2015. Exploratory data analysis using random forests, 73rd annual MPSA conference,
489 April 16-19, 2015, Chicago, United States of America.

490 URL <https://pdfs.semanticscholar.org/e7b7/3565b07a7f1369a20b1055f222423f0feb34.pdf>

491 Laybourn-Langton, L., Quilter-Pinner, H., Ho, H., 2016. Lethal and illegal: Solving london’s air pollution
492 crisis, institute for Public Policy Research.

493 URL <http://www.ippr.org/read/lethal-and-illegal-solving-londons-air-pollution-crisis>

494 Libiseller, C., Grimvall, A., Waldén, J., Saari, H., 2005. Meteorological normalisation and non-parametric
495 smoothing for quality assessment and trend analysis of tropospheric ozone data. *Environmental Monitoring*
496 *and Assessment* 100 (1), 33–52.

497 URL <http://dx.doi.org/10.1007/s10661-005-7059-2>

498 Lyubchich, V., Gel, Y. R., El Shaarawi, A., 2013. On detecting non-monotonic trends in environmental time
499 series: a fusion of local regression and bootstrap. *Environmetrics* 24 (4), 209–226.

500 URL <http://dx.doi.org/10.1002/env.2212>

501 Monks, P., Granier, C., Fuzzi, S., Stohl, A., Williams, M., Akimoto, H., Amann, M., Baklanov, A.,
502 Baltensperger, U., Bey, I., Blake, N., Blake, R., Carslaw, K., Cooper, O., Dentener, F., Fowler, D.,
503 Fragkou, E., Frost, G., Generoso, S., Ginoux, P., Grewe, V., Guenther, A., Hansson, H., Henne, S.,
504 Hjorth, J., Hofzumahaus, A., Huntrieser, H., Isaksen, I., Jenkin, M., Kaiser, J., Kanakidou, M., Klimont,
505 Z., Kulmala, M., Laj, P., Lawrence, M., Lee, J., Liousse, C., Maione, M., McFiggans, G., Metzger, A.,
506 Mieville, A., Moussiopoulos, N., Orlando, J., O’Dowd, C., Palmer, P., Parrish, D., Petzold, A., Platt, U.,
507 Pschl, U., Prvt, A., Reeves, C., Reimann, S., Rudich, Y., Sellegri, K., Steinbrecher, R., Simpson, D.,
508 ten Brink, H., Theloke, J., van der Werf, G., Vautard, R., Vestreng, V., Ch. Vlachokostas, von Glasow,
509 R., 2009. Atmospheric composition change - global and regional air quality. *Atmospheric Environment*
510 43 (33), 5268 – 5350.

511 URL <http://www.sciencedirect.com/science/article/B6VH3-4X3N46N-1/2/>

512 [1db0fa3c5afafc9418ab227802a71755](https://doi.org/10.1db0fa3c5afafc9418ab227802a71755)

513 NOAA, 2016. Integrated Surface Database (ISD).

514 URL <https://www.ncdc.noaa.gov/isd>

515 R Core Team, 2018. R: A Language and Environment for Statistical Computing. R Foundation for Statistical
516 Computing, Vienna, Austria.

517 URL <https://www.R-project.org/>

518 Ricardo Energy & Environment, 2018. Kent air quality database.

519 URL <http://www.kentair.org.uk>

520 Schmidt, C. W., Jan. 2016. Beyond a One-Time Scandal: Europe's Ongoing Diesel Pollution Problem.
521 Environmental Health Perspectives 124 (1), A19–A22.

522 URL <http://www.ncbi.nlm.nih.gov/pmc/articles/PMC4710587/>

523 Stull, R. B., 1988. An Introduction to Boundary Layer Meteorology. Kluwer Academic Publishers, London.

524 Tong, W., Hong, H., Fang, H., Xie, Q., Perkins, R., Mar. 2003. Decision forest: Combining the predictions
525 of multiple independent decision tree models. Journal of Chemical Information and Computer Sciences
526 43 (2), 525–531.

527 URL <http://dx.doi.org/10.1021/ci020058s>

528 Transport for London, 2018. Driving.

529 URL <https://tfl.gov.uk/modes/driving/>

530 Weiss, M., Bonnel, P., Kühlwein, J., Provenza, A., Lambrecht, U., Alessandrini, S., Carriero, M., Colombo,
531 R., Forni, F., Lanappe, G., Le Lijour, P., Manfredi, U., Montigny, F., Sculati, M., Dec. 2012. Will Euro
532 6 reduce the NO_x emissions of new diesel cars? — Insights from on-road tests with Portable Emissions
533 Measurement Systems (PEMS). Atmospheric Environment 62, 657–665.

534 URL <http://www.sciencedirect.com/science/article/pii/S1352231012008412>

535 Westmoreland, E. J., Carslaw, N., Carslaw, D. C., Gillah, A., Bates, E., Dec. 2007. Analysis of air quality
536 within a street canyon using statistical and dispersion modelling techniques. Atmospheric Environment
537 41 (39), 9195–9205.

538 URL <http://www.sciencedirect.com/science/article/pii/S1352231007006863>

539 Wise, E. K., Comrie, A. C., Aug. 2005. Extending the Kolmogorov–Zurbenko Filter: Application to Ozone,
540 Particulate Matter, and Meteorological Trends. Journal of the Air & Waste Management Association
541 55 (8), 1208–1216.

542 URL <http://dx.doi.org/10.1080/10473289.2005.10464718>

543 Zeileis, A., Kleiber, C., Krämer, W., Hornik, K., Oct. 2003. Testing and dating of structural changes in
544 practice. Computational Statistics & Data Analysis 44 (1–2), 109–123.

545 URL <http://www.sciencedirect.com/science/article/pii/S0167947303000306>

546 Zeileis, A., Leisch, F., Hornik, K., Christian, K., 2002. **strucchange**: An R Package for Testing for Structural
547 Change in Linear Regression Models. *Journal of Statistical Software* 7 (2), 1–38.
548 URL <http://www.jstatsoft.org/v07/i02/>
549 Ziegler, A., König, I. R., Dec. 2013. Mining data with random forests: current options for real-world
550 applications. *WIREs Data Mining and Knowledge Discovery* 4 (1), 55–63.
551 URL <https://doi.org/10.1002/widm.1114>

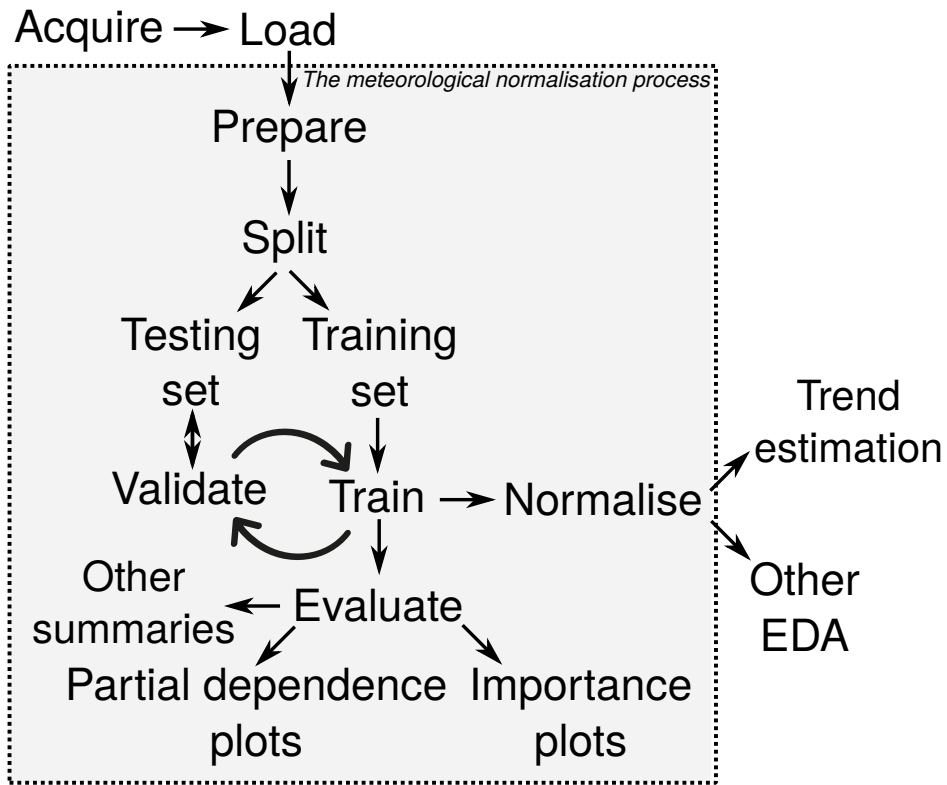


Figure A1: The framework for the meteorological normalisation technique. The training and validation phase is iterative to ensure the model does not overfit and adequate performance is achieved. After the technique has been completed, other analyses are conducted on the normalised time series.

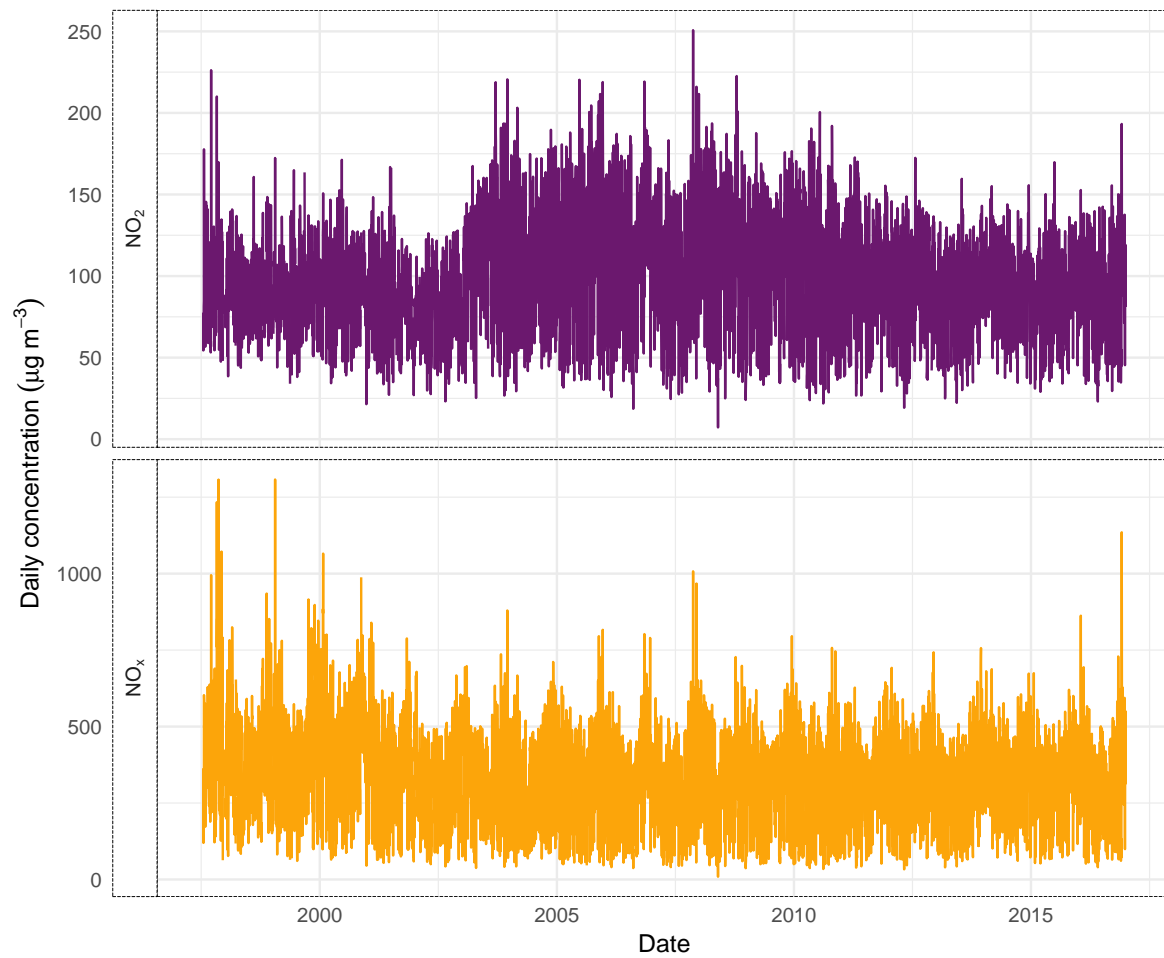


Figure A2: Daily NO₂ and NO_x concentrations at London Marylebone Road between 1997 and 2016.

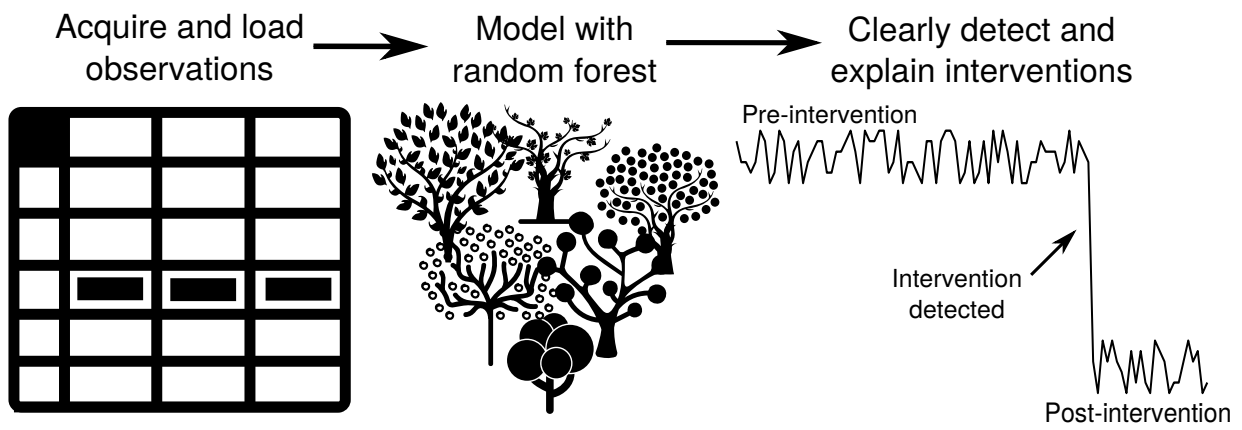


Figure A3: Graphical abstract. Icons designed by freepik.com from Flaticon.